ELSEVIER

Journal of Photochemistry and Photobiology A: Chemistry 105 (1997) 337–343

Journal of PHOTOCHEMISTRY AND PHOTOBIOLOGY A: CHEMISTRY

Excited state intramolecular charge transfer rates of *p*-dimethylaminobenzonitrile (DMABN) in solution: a two-dimensional dynamics perspective

Hyung J. Kim [a,*], James T. Hynes [b,*,1]

[a] *Department of Chemistry, Carnegie Mellon University, 4400 Fifth Ave., Pittsburgh, PA 15213-2683, USA*

[b] *Service de Chimie Moléculaire, CEA/Saclay, DSM/DRECAM/URA 331 CNRS, 91191 Gif-sur-Yvette, France*

Received 25 August 1996; accepted 18 October 1996

Abstract

The two-dimensional formulation, in the twist angle and a solvent coordinate, of the photoreaction dynamics of *p*-dimethylaminobenzonitrile (DMABN) in solution of Fonseca et al. (*J. Mol. Liq., 60* (1994) 161) is implemented with the aid of recently available vacuum quantum chemistry calculations and is extended to include direct dissipative frictional effects on each coordinate. Good agreement is found with recent experimental rate measurements for DMABN in acetonitrile, methanol and ethanol solvents. © 1997 Elsevier Science S.A.

Keywords: *p*-Dimethylaminobenzonitrile; Excited state intramolecular charge transfer; Two-dimensional dynamics; TICT; Solvent effects

1. Introduction

The excited electronic state photoreaction of *p*-dimethylaminobenzonitrile (DMABN) in solution [1], which led to the introduction of the twisted intramolecular charge transfer (TICT) concept [2], has been the object of extensive experimental and theoretical inquiry and ongoing controversy. (For reviews and papers with extensive reference listings, see Refs. [3–10].) Briefly, in the TICT scenario, the excited state DMABN photoreaction is supposed to involve a twisting motion in the terminal dimethylamino group to produce a highly polar/twisted charge transfer state, stabilized by a polar solvent. This scenario has also been invoked for many other molecules [2–5,8,10]. However, it is a measure of the unresolved character of DMABN and related molecule photoreactions that alternative reaction mechanisms have been proposed [5], continuing to the present [10].

This contribution continues and extends earlier work by Fonseca et al. [6,7] on the DMABN photoreaction in solution and focuses on issues of the reaction paths and rates. Indeed, it is important to emphasize, especially given the significant and extensive gas phase experimental and theoretical work on this and related systems in recent years, that the DMABN reaction occurs only in solution and not in vacuum, so that solution rate issues must be addressed (see Ref. [9] for a recent overview from this perspective). In this paper, we again employ a two-dimensional perspective, involving both the twist coordinate and a solvent coordinate as in Refs. [6,7]; the latter allows an account of the critical non-equilibrium solvation conditions relevant for the reaction, in contrast with the equilibrium solvation reaction field methods often employed. Compared with Refs. [6,7], there are three new features. First, we employ more recent and higher level vacuum quantum chemical calculations [8] in order to construct a two valence bond (VB) state description for the solution problem. Second, we extend the analysis of Refs. [6,7] to include direct solvent dissipative frictional damping on the twist and solvent coordinates, features necessary to discuss explicitly the impact of the viscosity and the solvation time of the solvent on the reaction rates. By the inclusion of both the inertial and dissipative solvation dynamics, our approach goes beyond previous efforts via various overdamped solvent descriptions with the inertial component neglected [11–14]. Finally, we compare our theoretical rate results with recently available experimental data due to Changenet et al. [15].

As in Refs. [6,7], we restrict our attention to activated DMABN reactions, with barrier heights of approximately a few kilocalories per mole, such that exponential time kinetics are experimentally observed; these conditions are satisfied for the three solvents considered here, acetonitrile, methanol

* Corresponding author.

[1] Permanent address: Department of Chemistry and Biochemistry, University of Colorado, Boulder, CO 80309-0215, USA.

PII S1010-6030(96)04543-1

and ethanol, all at room temperature [15]. The barrierless case (or nearly so), with non-exponential time kinetics [11,16,17], represents a different physical situation which should be clearly distinguished from the activated case and calls for a different treatment of the rate aspects.

2. Theory and model

We begin with a brief summary of the theoretical formulation of Ref. [6], relevant for TICT reactions. Except for some technical details on the cavity boundary effects, the non-equilibrium free energy description employed here is exactly the same as in our previous study. Thus we repeat only the formulae essential to establishing our notation and also to studying dissipative dynamics later on. For details, the reader is referred to Ref. [6].

As in Refs. [6,7], we assume that the excited state electron transfer for a TICT molecule is characterized by two orthogonal diabatic VB states, a locally excited (LE) state $\psi_{le}(\theta)$ and a charge transfer (CT) state $\psi_{ct}(\theta)$, where θ is the twist angle. (For DMABN, this is the angle between the amino group and the phenyl ring.) The solute wavefunction is described as a linear combination of these two basis functions, with coefficients which vary with both θ and the solvent polarization configuration. In this basis, the vacuum electronic hamiltonian $\hat{H}^0$ relevant for TICT dynamics is given by a 2×2 matrix

$$\hat{H}^0=\begin{bmatrix} E^0_{le}(\theta) & -\beta(\theta) \\ -\beta(\theta) & E^0_{ct}(\theta) \end{bmatrix} \tag{1}$$

where E^0_{le} and E^0_{ct} are the vacuum diabatic energies for the LE and CT states respectively and β is the effective electronic coupling between the two. With regard to the solute electric field, it is assumed to be that of a point dipole in either electronic configuration, so that

$$\hat{\epsilon}=-\nabla\frac{\vec{r}\cdot\hat{p}}{r^3};\ \hat{p}=\begin{bmatrix} \vec{\mu}_{le}(\theta) & 0 \\ 0 & \vec{\mu}_{ct}(\theta) \end{bmatrix} \tag{2}$$

where $\hat{p}$ is the solute dipole operator and $\vec{r}$ is a point in the solvent medium with the point dipole at the origin. In Eq. (2), we have neglected the transition dipole moment between the two diabatic states. Both $\hat{H}^0$ and $\hat{p}$ depend on θ.

As pointed out in Refs. [6,7], for a typical TICT system, the characteristic timescale for the excited state electron transfer is much slower than that for the solvent electronic polarization $\vec{P}_{el}$. We can then safely invoke the Born–Oppenheimer approximation for $\vec{P}_{el}$, so that the combined solute–solvent system is described by an effective hamiltonian operator $\hat{H}$

$$\hat{H}=\hat{H}^0-\frac{1}{2}R_\infty\hat{p}^2-R_{or}\vec{m}\cdot\hat{p}+\frac{1}{2}R_{or}\vec{m}^2 \tag{3}$$

where $\vec{m}$ is a dipole vector which efficiently gauges arbitrary solvent orientational polarization $\vec{P}_{or}$ coupled to the dipolar solute electric field

$$\vec{P}_{or}=\frac{3}{4\pi}\frac{\epsilon_\infty-\epsilon_0}{2\epsilon_0+1}\nabla\frac{\vec{m}\cdot\vec{r}}{r^3} \tag{4}$$

and R_∞ and R_{or} denote the reaction field factors associated with $\vec{P}_{el}$ and $\vec{P}_{or}$ respectively

$$R_\infty=\frac{2(\epsilon_\infty-1)}{2\epsilon_\infty+1}\frac{1}{a^3};\ R_{or}=\frac{6(\epsilon_0-\epsilon_\infty)}{(2\epsilon_\infty+1)(2\epsilon_0+1)}\frac{1}{a^3} \tag{5}$$

in the presence of a spherical cavity of radius a. The corresponding equilibrium reaction field factor R_{eq} is given by

$$R_{eq}=R_\infty+R_{or}=\frac{2(\epsilon_0-1)}{2\epsilon_0+1}\frac{1}{a^3} \tag{6}$$

where ϵ_0 and ϵ_∞ are the static and optical dielectric constants of the solvent medium respectively. We note that, due to the explicit account of cavity boundary effects on both $\vec{P}_{el}$ and $\vec{P}_{or}$ [18], the appropriate dipole reaction field factors appear in Eq. (3); this is to be contrasted with our previous study [6,7] where the dielectric image effects were neglected.

Following Refs. [6,7,19], we introduce a scalar solvent coordinate s as

$$\vec{m}=s\,\vec{\mu}_0+\vec{\mu}_1 \tag{7}$$

where $\vec{\mu}_0$ and $\vec{\mu}_1$ are conveniently chosen dipole vectors (see Eq. (11) below). The effective hamiltonian $\hat{H}$ then becomes

$$\hat{H}=\begin{bmatrix} G_{le}(\theta,s) & -\beta(\theta) \\ -\beta(\theta) & G_{ct}(\theta,s) \end{bmatrix} \tag{8}$$

where the diabatic free energies in solution are

$$G_{le}(\theta,s)=E^0_{le}(\theta)-\frac{1}{2}R_{eq}\mu^2_{le}(\theta)+\frac{1}{2}R_{or}\{s\,\mu_0+\mu_1-\mu_{le}(\theta)\}^2 \tag{9a}$$

$$G_{ct}(\theta,s)=E^0_{ct}(\theta)-\frac{1}{2}R_{eq}\mu^2_{ct}(\theta)+\frac{1}{2}R_{or}\{s\,\mu_0+\mu_1-\mu_{ct}(\theta)\}^2 \tag{9b}$$

By diagonalizing $\hat{H}$, we can obtain two adiabatic excited electronic states in solution, together with their free energies as a function of θ and s. In particular, the lower state defines the electronically adiabatic free energy surface on which TICT dynamics occur via the solute twist and solvent polarization fluctuation motions. The details of the adiabatic states and associated equilibrium solvation states are given in Refs. [6,7] and thus will not be repeated here.

We now apply the formulation above to study the excited state electron transfer for DMABN. As in Refs. [6,7], we employ a semiempirical approach; to be specific, we determine the parameters associated with the two vacuum VBs and the solvent by using existing ab initio quantum chemistry results and also experimental information on static electronic spectroscopy. Compared with the vacuum calculations of

Kato and Amatatsu [20], employed in Refs. [6,7] to generate the vacuum VB states (an LE state and a CT state) as a function of the twist angle θ, the more recent higher level complete active space self-consistent field (CASSCF) with multiconfigurational second-order perturbation theory (CASPT2) of Serrano-Andrés et al. [8] shows qualitative differences, e.g. a CT curve decreasing in energy with θ, and we regenerate the VB curves on the basis of the latter calculations. In the model calculations, the following vacuum diabatic energies (kcal mol^{-1}) and dipole moments (D) are employed (Fig. 1)

$$E^0_{le}(\theta) = 13 \sin^2\theta;\ E^0_{ct}(\theta) = -1.5 \sin^2\theta + 13;$$
$$\mu_{le}(\theta) = 7;\ \mu_{ct}(\theta) = 2 \sin^2\theta + 13 \quad (10)$$

where both the LE and CT dipoles are parallel to the DMABN molecular axis. Since the LE dipole moment does not change with θ in our model description, we choose the following values for μ_0 and μ_1 in Eq. (7)

$$\mu_0 = \mu_{ct}(\theta = 0) - \mu_{le} = 6;\ \mu_1 = \mu_{le} = 7 \quad (11)$$

For the electronic coupling, we use

$$\beta(\theta) = 1.8 \cos^2\theta + 0.2 \text{ (kcal mol}^{-1}\text{)} \quad (12)$$

which is slightly smaller than our previous value [6,7]. We regard β as an effective coupling averaged over symmetry-breaking vibrations, including the amino group pyramidalization coordinate (see Ref. [6] for discussion).

We also need the cavity size a for the reaction field factors (Eq. (5) and Eq. (6)). In the present work, we employ $a = 4.3$ Å. This value, together with Eq. (10), reproduces the experimentally observed approximately 2.3 kcal mol^{-1} red shift of the DMABN CT absorption band when the solvent is changed from *n*-heptane to diethyl ether [5,8].

With these parameters, we can obtain the two-dimensional adiabatic free energy surface $G_1(\theta,s)$ for DMABN in a straightforward manner. The results in acetonitrile and methanol solvents are shown in Fig. 2. The ethanol solvent result is qualitatively similar and is not shown. These surfaces are qualitatively similar to the results of Refs. [6,7]. The barrier heights $\Delta G^{\ddagger}$ and reaction free energies ΔG_{rxn} are collected in Table 1.

Also shown on the surfaces of Fig. 2 are the reaction paths, the solution analogs [19] of the gas phase Fukui intrinsic reaction coordinate [29]. As in Refs. [6,7], the reaction path is mainly in the twist coordinate for CH_3CN; due to the low value of the solvent frequency $\omega_s = (G_1^{ss}/m_s)^{1/2} = 8.3$ ps^{-1} (the solvent frequency is connected with inertial effects in

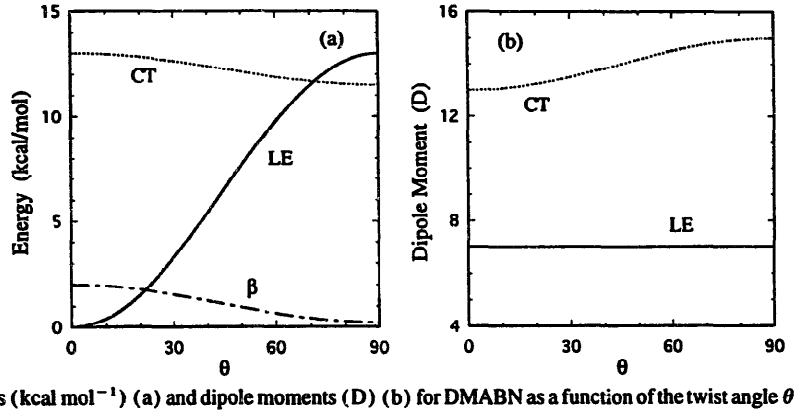

Fig. 1. Vacuum diabatic energies (kcal mol^{-1}) (a) and dipole moments (D) (b) for DMABN as a function of the twist angle θ (degrees). Their parametrization is couched in terms of recent CAS quantum chemistry calculations [8]. The electronic coupling is essentially the same as in our previous study [6,7], except that its overall magnitude is reduced by 0.2 kcal mol^{-1} or less.

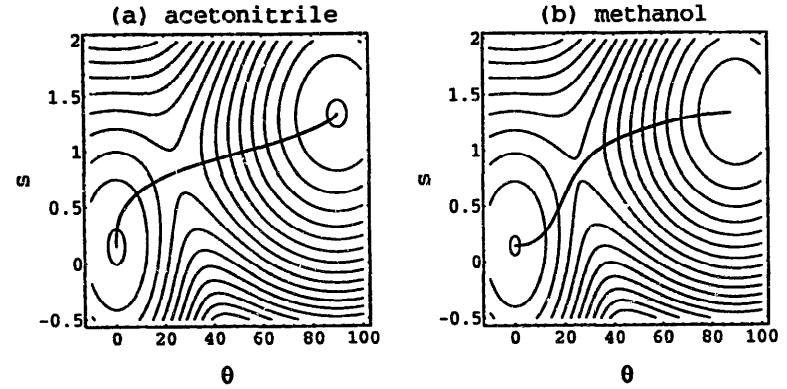

Fig. 2. Adiabatic free energy contour diagrams for DMABN in acetonitrile (a) and methanol (b). The free energy difference for two nearby contour lines is 0.5 kcal mol^{-1}. The reaction paths for excited state electron transfer are also shown. The solvent frequencies employed in the calculations are $\omega_s = 8.3$ ps^{-1} for acetonitrile and $\omega_s = 30$ ps^{-1} for methanol, while the solute torsional frequency along θ in vacuum is assumed to be 14 ps^{-1} (cf. Ref. [21]). For both (a) and (b), the reaction path smoothly connects the reactant and product states, located near (0°, 0.14) and (90°, 1.33) respectively.

Table 1
Parameters and calculated results for DMABN [a]

Solvent	ϵ_0	ϵ_∞	η [b]	Ω_ζ	ω_s [c]	τ_s [d]	$\omega_{b,eq}$	$\Delta G^\ddagger$	ΔG_{rxn}
CH_3CN	35.9	1.81	0.35	10	8.3	0.25	18.3	1.5	−3.0
CH_3OH	32.7	1.77	0.60	20	30	5	18.5	1.5	−2.9
C_2H_5OH	24.6	1.85	1.20	30	16	17	18.6	1.6	−2.7

[a] The units for the viscosity, frequency, time and free energy are cP, ps^{-1}, ps and kcal mol^{-1} respectively.
[b] From Ref. [22] ($T=20$ °C for methanol and ethanol and $T=25$ °C for acetonitrile).
[c] From Ref. [23] for acetonitrile and from Refs. [24,25] for methanol. For ethanol, the frequency was determined from the methanol value $\omega_s=30$ ps^{-1} appropriately scaled by the factor 0.54, i.e. the ratio of the ethanol and methanol frequencies estimated from Ref. [27].
[d] From Refs. [26–28].

time-dependent fluorescence (TDF) in Section 3), the solvent cannot keep up in the rapid passage over the saddle point (‡) in the surface, and must extensively rearrange prior to this passage. On the other hand, methanol is a comparatively fast solvent ($\omega_s=30$ ps^{-1}), and the reaction coordinate through the transition state region heavily involves solvent motion. Two points are important here. The first is that, even in the methanol case, where the reaction coordinate is predominantly the solvent, there is no barrier on the two-dimensional surface along the line $s=s^\ddagger$, i.e. the DMABN reaction is not like an activated outer-sphere electron transfer reaction. Second, the characterization of the solvents above as fast or slow (ethanol with $\omega_s=16$ ps^{-1} is intermediate; the ethanol frequency is determined from the methanol value $\omega_s=30$ ps^{-1}, appropriately scaled by the factor 0.54, i.e. the ratio of the ethanol and methanol frequencies estimated from Ref. [27]) is based on the relevant short-time, inertial characteristic timescales of the solvents. When viewed on a longer timescale, methanol and ethanol would be considered as slow relative to acetonitrile since the integrated solvation times for the former, as determined in TDF [26–28,30], far exceed that of the latter. The role of the solvation time is taken up in Section 3.

Finally, although we do not present the data here, we have confirmed, by calculations which include variation of the solvent dielectric constant, the important approximately linear trends of the activation free energy $\Delta G^\ddagger$ with the solvent polarity (Pekar factor) and the reaction thermodynamics (ΔG_{rxn}) found in Refs. [6,7] and consistent with the experimental results of Eisenthal and coworkers [31], stressing again the all-important variation of the DMABN reaction barrier height with the static solvent polarity [31,32].

3. Reaction rate constants

The most common description of the reaction rate constant is that of equilibrium solvation, in which it is imagined that the solvent is equilibrated at each value of the twist angle θ. Then the rate constant is [6,7]

$$k_{ES}=\frac{\omega^R_{\theta,eq}}{2\pi}\frac{\omega^R_s}{\omega^\ddagger_s}\exp(-\Delta G^\ddagger/k_BT) \tag{13}$$

where $\Delta G^\ddagger$ is the activation free energy on the (θ,s) surface, the first prefactor contains the equilibrium θ well frequency in the reactant (R) configuration and the ratio of the transverse solvent frequencies at R and ‡ is related to an entropic effect on the rate.

Even in the absence of dissipative effects on the θ and s motions, a two-dimensional transition state theory (TST) rate constant is generally less than k_{ES} due to the lack of equilibrium solvation. Such a rate constant

$$k_{ND}=\frac{\omega^R_\parallel}{2\pi}\frac{\omega^R_\perp}{\omega^\ddagger_\perp}\exp(-\Delta G^\ddagger/k_BT) \tag{14}$$

involving the parallel (‖) and perpendicular (⊥) frequencies for the surface in the reactant and transition state regions has been derived and discussed previously [6,7]. For our present purposes, we simply observe that Eq. (14) includes dynamic solvation effects at the non-dissipative level, which in TDF dynamics will correspond to the inertial, gaussian initial dynamics [23–25,33–35], i.e. $\exp(-\omega_s^2t^2/2)$, where ω_s is the solvent frequency.

To such a description, we now add dissipative frictional effects for both the θ and s coordinates such that, in the neighborhood of the saddle point, the equations of motion are

$$I_\theta\delta\ddot{\theta}(t)=-G_1^{\theta\theta}\delta\theta(t)-G_1^{\theta s}\delta s(t)-I_\theta\int_0^t d\tau\zeta_{\theta\theta}(t-\tau)\delta\dot{\theta}(\tau) \tag{15}$$

$$m_s\delta\ddot{s}(t)=-G_1^{\theta s}\delta\theta(t)-G_1^{ss}\delta s(t)-m_s\int_0^t d\tau\zeta_{ss}(t-\tau)\delta\dot{s}(\tau) \tag{16}$$

where δ denotes the deviations of the variables from their transition state values, i.e. $\delta\theta=\theta-\theta^\ddagger$ and $\delta s=s-s^\ddagger$, and inessential "random force" terms have been suppressed. Here the various surface second derivative terms (e.g. $G_1^{ss}=\partial^2G_1/\partial s^2|_\ddagger=m_s\omega_s^2$) previously treated [6,7] have been supplemented by the two dissipative frictional terms, one for each coordinate, to be specified below.

As in other work [36], Eq. (15) and Eq. (16) can be simultaneously formally solved in Laplace transform language to produce an equivalent one-dimensional generalized Langevin equation (GLE) for the twist coordinate

$$\delta\ddot{\theta}(t) = \omega_{b,eq}^2\theta(t) - \int_0^t d\tau\zeta_\theta(t-\tau)\delta\dot{\theta}(\tau) \quad (17)$$

in which $\omega_{b,eq}$ is the equilibrium barrier frequency in θ, i.e. with the solvent equilibrated to θ

$$\omega_{b,eq}^2 = -\frac{1}{I_\theta}\left(G_1^{\theta\theta} - \frac{(G_1^{\theta s})^2}{G_1^{ss}}\right) \quad (18)$$

and the total time-dependent friction coefficient for the θ motion satisfies the Laplace transform relation

$$\hat{\zeta}_\theta(z) = \int_0^\infty dt\, e^{-zt}\zeta_\theta(t)$$

$$= \hat{\zeta}_{\theta\theta}(z) + \frac{m_s}{I_\theta}\frac{(G_1^{\theta s})^2}{\omega_s^2}\left[z + \frac{\omega_s^2}{z+\hat{\zeta}_{ss}(z)}\right]^{-1} \quad (19)$$

in which the last contribution arises from the free energy surface coupling, via $G_1^{\theta s}$, of the two coordinates. It is worth pointing out that the inverse bracket in Eq. (19) is the Laplace transform of the normalized time correlation function (TCF) of $\delta s(t)$ at the transition state and is analogous to the corresponding solvent dynamic functions in TDF [33].

With the GLE Eq. (17) for the twist coordinate in hand, the overall reaction rate constant, including dissipative friction, can be expressed via Grote–Hynes (GH) theory [37] as

$$k = \kappa k_{ES};\ \kappa = [\kappa + \omega_{b,eq}^{-1}\hat{\zeta}_\theta(z=\omega_{b,eq}\kappa)]^{-1} \quad (20)$$

If $\hat{\zeta}_\theta$ is neglected, $\kappa \to 1$ and $k = k_{ES}$ (Eq. (13)), whereas if the frictions $\hat{\zeta}_{\theta\theta}$ and $\hat{\zeta}_{ss}$ are neglected, $k \to k_{ND}$ (Eq. (14)), i.e. $\kappa \to k_{ND}/k_{ES}$.

As will be seen in more detail below, we only need the various frictions for the fairly high frequencies z comparable with the equilibrium barrier frequency $\omega_{b,eq}$, so that a complete description on the longest timescales is not required. Accordingly, for the direct θ coordinate friction $\zeta_{\theta\theta}(t)$, we adopt a short-time gaussian description via a route recently developed by one of us [35], according to which

$$\hat{\zeta}_{\theta\theta}(z) \approx \frac{\sqrt{\pi}}{4}\Omega_\zeta e^{z^2/\Omega_\zeta^2}\,\mathrm{erfc}\frac{z}{\Omega_\zeta} \quad (21)$$

where erfc is the complementary error function and the frequency Ω_ζ is determined from the short-time behavior of the angular velocity autocorrelation function, i.e. $\exp[-\Omega_\zeta^2 t^2/2]$. It was found in Ref. [35] that Eq. (21) reproduces the simulation results of $\hat{\zeta}_{\theta\theta}(z)$ for model dipolar solutes in water reasonably well. For DMABN in acetonitrile and alcohol solvents, we proceed as follows. According to a very recent molecular dynamics simulation study of model dipolar solutes in acetonitrile [38], $\Omega_\zeta/\sqrt{2}$ ranges from 5 to 15 ps^{-1}. We thus choose $\Omega_\zeta = 10$ ps^{-1} for CH_3CN. Recognizing that $\hat{\zeta}_{\theta\theta}(z=0) = (\sqrt{\pi}/4)\Omega_\zeta$ and assuming that the integrated short-time friction $\hat{\zeta}_{\theta\theta}(z=0)$ is proportional to the solvent viscosity η [39], we find from the η data in Table 1 that $\Omega_\zeta \approx 20$ ps^{-1} for methanol and approximately 30 ps^{-1} for ethanol. This completely determines the direct rotational friction needed for model calculations in all three solvents.

Secondly, we adopt the simplest description for the direct friction on the solvent coordinate

$$\hat{\zeta}_{ss}(z) = \zeta_{ss} = \omega_s^2\tau_s \quad (22)$$

i.e. a frequency-independent value, where τ_s is the solvation time available from TDF experiments [26–28,30]. This approximation corresponds to a Langevin equation description for the solvent variable δs itself [33,36,40]. Various parameters for the calculations are collected in Table 1.

The results for the reaction times $\tau_{rxn} = k^{-1}$ for DMABN in CH_3CN, CH_3OH and CH_3CH_2OH solvents are given in Table 2, where it is seen that the agreement with the experimental results of Changenet et al. [15] is quite striking. Rather than dwell on this aspect, we prefer to use comparison calculations to make several general points.

The first follows from the Kramers (KR) theory [41] entries for the reaction times in Table 2. Here the frequency dependence of $\hat{\zeta}_\theta$ is ignored, such that the solvent dynamic effect on the twisting motion is described as overdamped

$$\zeta_\theta = \hat{\zeta}_{\theta\theta}(z=0) + \frac{m_s}{I_\theta}\frac{(G_1^{\theta s})^2}{\omega_s^2}\tau_s \quad (23)$$

For the alcohol solvents, for which τ_s is large, this translates to an overdamped diffusive crossing of the barrier itself in the Kramers description and a dramatic overestimation of the reaction time (Table 2) due to an inappropriately predicted tracking by τ_{rxn} of the lengthening solvation time τ_s. Instead,

Table 2
Theoretical and experimental reaction times [a,b]

Solvent	τ_{exp} [c]	τ [d]	τ (with tail) [e]	τ_{KR} [f]	τ_{ES} [g]	τ_{ND} [h]
CH_3CN	6	6.5	6.7	18.6	4.7	6.0
CH_3OH	8	8.1	8.5	356	4.9	5.4
C_2H_5OH	12	11.0	11.8	1.3×10^3	5.9	6.9

[a] Units: ps^{-1}.
[b] Theoretical times are reported as the inverse of the rate constants, e.g. $\tau = k^{-1}$.
[c] From Ref. [15] with estimated uncertainties of ± 1 ps.
[d] GH results from Eq. (20). The corresponding reaction times with a Markovian direct friction on θ, i.e. $\zeta_{\theta\theta}(t) = \frac{\sqrt{\pi}}{2}\Omega_\zeta\delta(t)$, are 7.2, 9.2 and 12.5 ps respectively, indicating that it is important to account for the non-Markovian character of $\zeta_{\theta\theta}(t)$.
[e] With the slowly decaying friction Eq. (24) included.
[f] From Eq. (20) with $\hat{\zeta}_\theta(z=0)$.
[g] From Eq. (13). Comparison with τ indicates the importance of non-equilibrium contributions.
[h] From Eq. (14). Comparison with τ indicates the contribution of the dissipative frictions.

the GH predictions, consonant with the experimental results, give no such tracking: the relevant dynamics for the barrier crossing are on the short timescale $(\kappa\omega_{b,eq})^{-1} \sim \omega_{b,eq}^{-1} \sim$ 50 fs and the slow solvation dynamics are irrelevant.

It is worth making this point in another way. It is seen from Table 1 and Table 2 that both theoretically and experimentally the reaction time τ_{rxn} for DMABN in ethanol is shorter than the solvation time $\tau_s \approx 17$ ps. This is an impossibility if we take the strongly overdamped solvation point of view, in which $\tau_{rxn} \propto \tau_s$. However, the analysis above shows that the latter is simply an incorrect description.

Finally, it is important for clarity to stress that the analysis of the direct friction $\zeta_{\theta\theta}(t)$ in Section 2 is only reasonable for solvents of relatively low viscosity as in this paper. This friction is of a short-time "collisional" character and does not include a further long-lived "tail" contribution which would be important for high viscosity solvents, such as glycerol [42], and would lead to adherence to something like a Debye–Stokes relation ($\zeta_{\theta\theta} \propto \eta a^3$) for the direct friction constant for the twisting motion. (By contrast, the arguments used to estimate $\zeta_{\theta\theta}(t)$ in Section 2 invoke only a generally observed similarity between collisional friction trends and the solvent viscosity for low viscosity solvents [39].) If such a collective, long-lived tail were to be present for DMABN reactions of barrier frequencies comparable with the present case ($\omega_{b,eq} \approx 18\,ps^{-1}$), it would not contribute to the effective friction on the reaction coordinate for precisely the same short timescale domination reasons that preclude a tracking of τ_s by τ_{rxn}, and τ_{rxn} would not decline proportionally with η^{-1}. To see this clearly, we have calculated the reaction time with a slowly decaying, long-time tail component $\zeta_{\theta\theta}^{LT}$

$$\zeta_{\theta\theta}^{LT}(t) = \Lambda \exp[-t/\tau_\Lambda] \tag{24}$$

added to the gaussian friction in Eq. (21). In the numerical calculations, we have used

$$\tau_\Lambda = 1\ \text{ps};\ \Lambda\ (\text{in ps}^{-2}) = \frac{25}{4}\frac{\Omega_t}{\Omega_t(\text{in CH}_3\text{CN})} \tag{25}$$

so that the tail contribution increases with Ω_t and thus with η. It should be noted that with Eq. (21) and Eq. (24), the latter accounts for more than 50% of the total integrated direct rotational friction $\hat{\zeta}_{\theta\theta}(z=0)$. Despite this, comparison of the τ results in Table 2 with and without $\zeta_{\theta\theta}^{LT}$ included shows that the low-frequency slowly varying friction does not play any significant role in the reaction; the barrier crossing characterized by the timescale $\omega_{b,eq}^{-1}$ is too fast for $\zeta_{\theta\theta}^{LT}$ to participate. This insensitivity [31] is important; a lack of a significant viscosity effect for the rate is not [9] an indication of the absence of large-amplitude twisting motion.

4. Conclusions

In this contribution, we have shown that the implementation of the theoretical framework of Fonseca et al. [6,7], together with the ab initio quantum chemistry results of Serrano-Andrés et al. [8] and extension to include direct frictional damping on the twist and solvent coordinates, gives rate constants for the DMABN photoreaction in good agreement with the recent experimental results of Changenet et al. [15] in acetonitrile, methanol and ethanol solvents. A fuller account of this work and application to the remaining solvents employed in Ref. [15] will be given elsewhere.

Acknowledgements

This work was supported in part by NSF Grants CHE 9412035 (H.J.K.) and CHE 9312267 (J.T.H.). We wish to thank Professor Mark Maroncelli for sending us the unpublished rotational dynamics simulation results in acetonitrile [38] and for helpful discussions on the frequencies of alcoholic solvents. We also thank Dr. Monique Martin, Orsay, for making the DMABN rate data available and for useful discussions. J.T.H. thanks the members of the Laboratoire de Photophysique et Photochimique (LPP) group at Saclay for their hospitality, where this work was completed in the summer of 1996 as a CNRS Directeur de Récherche Associé (Acte Chimique Elémentaire en Phase Liquide, GDR 1017). Finally, the spirit of the late Teresa Fonseca, who initiated the TICT project, continues to inspire the authors' work.

References

[1] E. Lippert, W. Lüder and H. Boos, in A. Mangini (ed.), *Advances in Molecular Spectroscopy*, Pergamon, Oxford, 1962.
[2] Z.R. Grabowski, K. Rotkiewicz, A. Siemiarczuk, D.J. Cowley and W. Baumann, *Nouv. J. Chim., 3* (1979) 443. J. Lipiński, H. Chojnacki, Z.R. Grabowski and K. Rotkiewicz, *Chem. Phys. Lett., 70* (1980) 449.
[3] W. Rettig, G. Wermuth and E. Lippert, *Ber. Bunsenges. Phys. Chem., 83* (1979) 692. W. Rettig and E. Lippert, *J. Mol. Struct., 61* (1980) 17.
[4] W. Rettig, *Angew. Chem., Int. Ed. Engl., 25* (1986) 971. E. Lippert, W. Rettig, V. Bonačić-Koutecký, F. Heisel and A. Miehé, *Adv. Chem. Phys., 68* (1987) 1. J. Michl and V. Bonačić-Koutecký, *Electronic Aspects of Organic Photochemistry*, Wiley, New York, 1990. W. Rettig, in N. Mataga, T. Okada and H. Masuhara (eds.), *Dynamics and Mechanisms of Photoinduced Transfer and Related Phenomena*, Elsevier, 1992.
[5] K.A. Zachariasse, T. von der Haar, A. Hebecker, U. Leinhos and W. Kühnle, *Pure Appl. Chem., 65* (1993) 1745. T. von der Haar, A. Hebecker, Y. Il'ichev, W. Kühnle and K.A. Zachariasse, in A. Tramer (ed.), *Fast Elementary Processes in Chemical and Biological Systems*, AIP, New York, 1996, p. 295.
[6] T. Fonseca, H.J. Kim and J.T. Hynes, *J. Mol. Liq., 60* (1994) 161.
[7] T. Fonseca, H.J. Kim and J.T. Hynes, *J. Photochem. Photobiol. A: Chem., 82* (1994) 67.
[8] L. Serrano-Andrés, M. Merchán, B.O. Roos and R. Lindh, *J. Am. Chem. Soc., 117* (1995) 3189.
[9] J.T. Hynes, *Rev. Port. Quím., 2* (1995) 12.
[10] A.L. Sobolewski and W. Domke, *Chem. Phys. Lett., 250* (1996) 428.
[11] S.-G. Su and J.D. Simon, *J. Chem. Phys., 89* (1988) 908.
[12] G.K. Schenter and C.B. Duke, *Chem. Phys. Lett., 176* (1991) 563.
[13] A. Polimeno, A. Barbon, P.L. Nordio and W. Rettig, *J. Phys. Chem., 98* (1994) 12 158.
[14] S. Hayashi, K. Ando and S. Kato, *J. Phys. Chem., 99* (1995) 955.

[15] P. Changenet, P. Plaza, M.M. Martin and Y.H. Meyer, Role of intermolecular torsion and solvent dynamics in the charge transfer kinetics in triphenylphosphine oxide derivatives and DMABM, submitted. P. Changenet, *Thesis*, Orsay University, France, 1996.
[16] S.-G. Su and J.D. Simon, *J. Phys. Chem., 93* (1989) 753.
[17] F. Heisel and J.A. Miehé, *Chem. Phys., 98* (1985) 233. F. Heisel, J.A. Miehé and J.M.G. Martinho, *Chem. Phys., 98* (1985) 243. F. Heisel and J.A. Miehé, *Chem. Phys. Lett., 128* (1986) 323.
[18] H.J. Kim, *J. Chem. Phys., 105* (1996) 6818, 6833.
[19] S. Lee and J.T. Hynes, *J. Chem. Phys., 88* (1988) 6853.
[20] S. Kato and Y. Amatatsu, *J. Chem. Phys., 92* (1990) 7241.
[21] J.A. Warren, E.R. Bernstein and J.I. Seeman, *J. Chem. Phys., 88* (1988) 871. V.H. Grassian, J.A. Warren, E.R. Bernstein and H.V. Secor, *J. Chem. Phys., 90* (1989) 3994. R. Howell, H. Petek, D. Phillips and K. Yoshihara, *Chem. Phys. Lett., 183* (1991) 249.
[22] R.C. West, D.R. Lide, M.J. Astle and W.H. Beyer (eds.), *Handbook of Chemistry and Science*, CRC, Boca Raton, FL, 70th edn., 1989.
[23] M. Maroncelli, *J. Chem. Phys., 94* (1991) 2084.
[24] P.V. Kumar and M. Maroncelli, *J. Chem. Phys., 103* (1995) 3038.
[25] T. Fonseca and B.M. Ladanyi, *J. Phys. Chem., 95* (1991) 2116.
[26] M. Maroncelli, *J. Mol. Liq., 57* (1993) 1.
[27] M. Maroncelli, P.V. Kumar, A. Papazyan, M.L. Horng, S.J. Rosenthal and G.R. Fleming, in Y. Gauduel and P.J. Rossky (eds.), *Ultrafast Reaction Dynamics and Solvent Effects*, AIP, New York, 1994, p. 310.
[28] M.L. Horng, J. Gardecki, A. Papazyan and M. Maroncelli, *J. Phys. Chem., 99* (1995) 17 311.
[29] K. Fukui, *J. Chem. Phys., 74* (1970) 4161; *Acc. Chem. Res., 14* (1981) 363.
[30] M.A. Kahlow, T.J. Kang and P.F. Barbara, *J. Chem. Phys., 88* (1988) 2372. M.A. Kahlow, W. Jarzeba, T.J. Kang and P.F. Barbara, *J. Chem. Phys., 90* (1989) 151.
[31] J. Hicks, M.T. Vandersall, Z. Babarogic and K. Eisenthal, *Chem. Phys. Lett., 116* (1985) 18. J. Hicks, M. Vandersall, E.V. Sitzmann and K. Eisenthal, *Chem. Phys. Lett., 135* (1987) 413.
[32] N.S. Park and D.H. Waldeck, *J. Phys. Chem., 94* (1990) 662.
[33] E.A. Carter and J.T. Hynes, *J. Chem. Phys., 94* (1991) 5961.
[34] B.D. Bursulaya, D.A. Zichi and H.J. Kim, *J. Phys. Chem., 99* (1995) 10 069.
[35] B.D. Bursulaya, D.A. Zichi and H.J. Kim, *J. Phys. Chem., 100* (1996) 1392.
[36] G. van der Zwan and J.T. Hynes, *J. Chem. Phys., 78* (1983) 4174; *Chem. Phys., 90* (1984) 21.
[37] R.F. Grote and J.T. Hynes, *J. Chem. Phys., 73* (1980) 2715.
[38] P.V. Kumar and M. Maroncelli, personal communication, 1996.
[39] R.F. Grote, G. van der Zwan and J.T. Hynes, *J. Phys. Chem., 88* (1984) 4676. J.T. Hynes, R. Kapral and M. Weinberg, *J. Chem. Phys., 69* (1978) 2725.
[40] G. van der Zwan and J.T. Hynes, *J. Phys. Chem., 89* (1985) 4181.
[41] H.A. Kramers, *Physica, 7* (1940) 284.
[42] D. Braun and W. Rettig, *Chem. Phys., 180* (1994) 231.